Science Advances
AAAS

Supplementary Materials for

MCJ: A mitochondrial target for cardiac intervention in pulmonary hypertension

Ayelén M. Santamans *et al.*

Corresponding author: Guadalupe Sabio, gsabio@cnic.es

Sci. Adv. **10**, eadk6524 (2024)
DOI: 10.1126/sciadv.adk6524

The PDF file includes:

Other Supplementary Material for this manuscript includes the following:

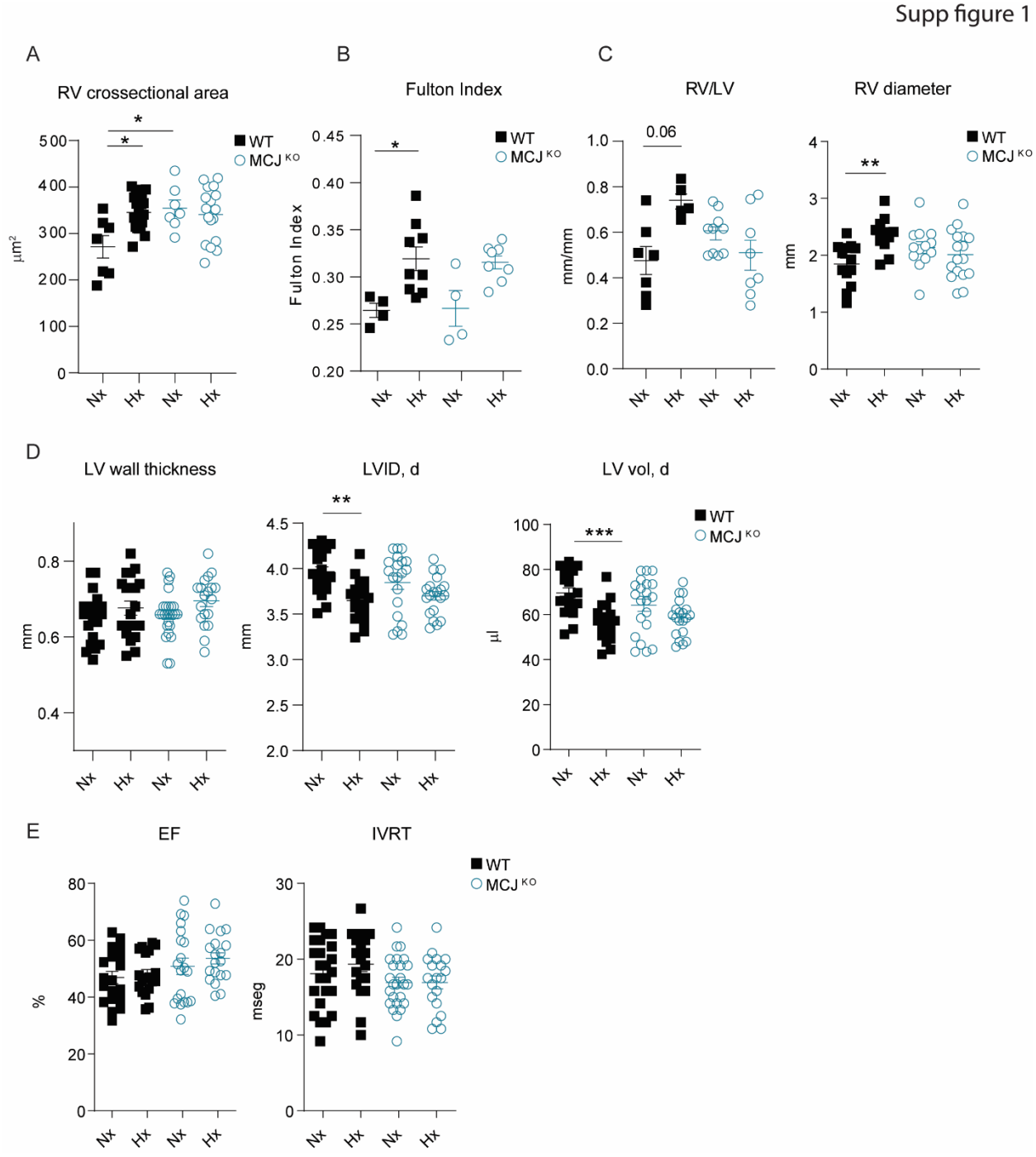

Fig. S1. MCJ deletion preserves RV and LV morphology and function after chronic hypoxia.

WT and MCJ^{KO} mice subjected to normoxia (Nx) or 28 days hypoxia (Hx, 10% O_2). **(A)** RV cardiomyocyte crossectional area by WGA immunostaining (n=7-18). **(B)** Fulton Index (n=4-9). **(C-E)** Echocardiography measured parameters in Nx and Hx: ratio between RV diameter/LV diameter; RV dilation shown as RV diameter; LV wall thickness (average of IVS; d and LVPW; d); LVID; d, left ventricular internal diameter in diastole; LV vol; d, left ventricular volume in

diastole; EF (%), ejection fraction; IVRT, isovolumetric relaxation time (n=12-22). All data are presented as mean ± s.e.m. Statistical comparison by two-way ANOVA with Tukey post-test (a,b,c,d,e): NS (non-significant),*P < 0.05, **P < 0.01, ***P < 0.001. IVS; d interventricular septum thickness in diastole; LVPW; d, left ventricle posterior wall thickness in diastole.

Supp figure 2

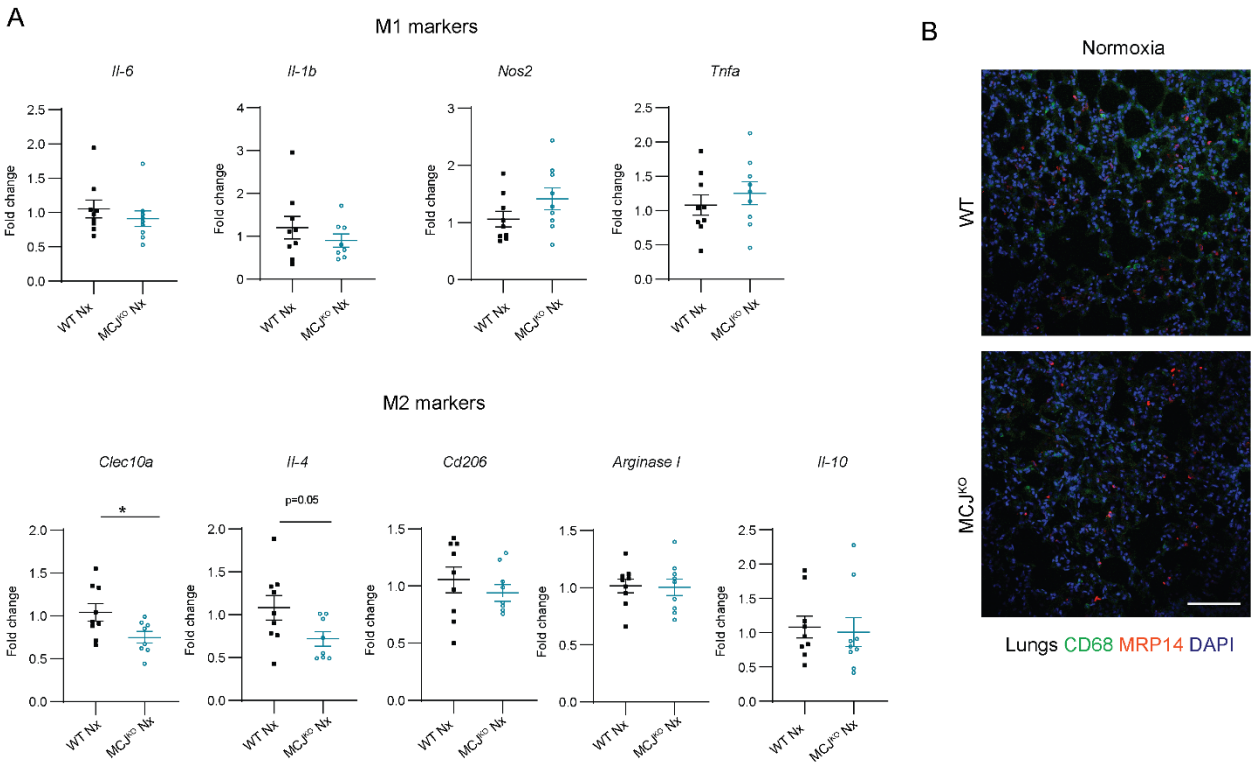

Fig. S2. Lack of MCJ does not influence the basal pulmonary immune cell infiltration or the M1/M2 profile.

(A) Lung expression profile of baseline M1 and M2 markers in WT and MCJ^{KO} mice (Nx, 21% O_2) analyzed by qPCR (n=8-9). The data is expressed as fold change relative to WT Nx; GAPDH expression levels were used to normalize the data. **(B)** Lung immunofluorescence showing infiltration by macrophages (CD68) and neutrophils (MRP14) in normoxic lungs. Nuclei stained with DAPI. Scale bar, 100 µm. All data are presented as mean ± s.e.m. Statistical comparison by student´s t-test (a): NS (nonsignificant), *P < 0.05, **P < 0.01, ***P < 0.001.

A

Supp figure 3

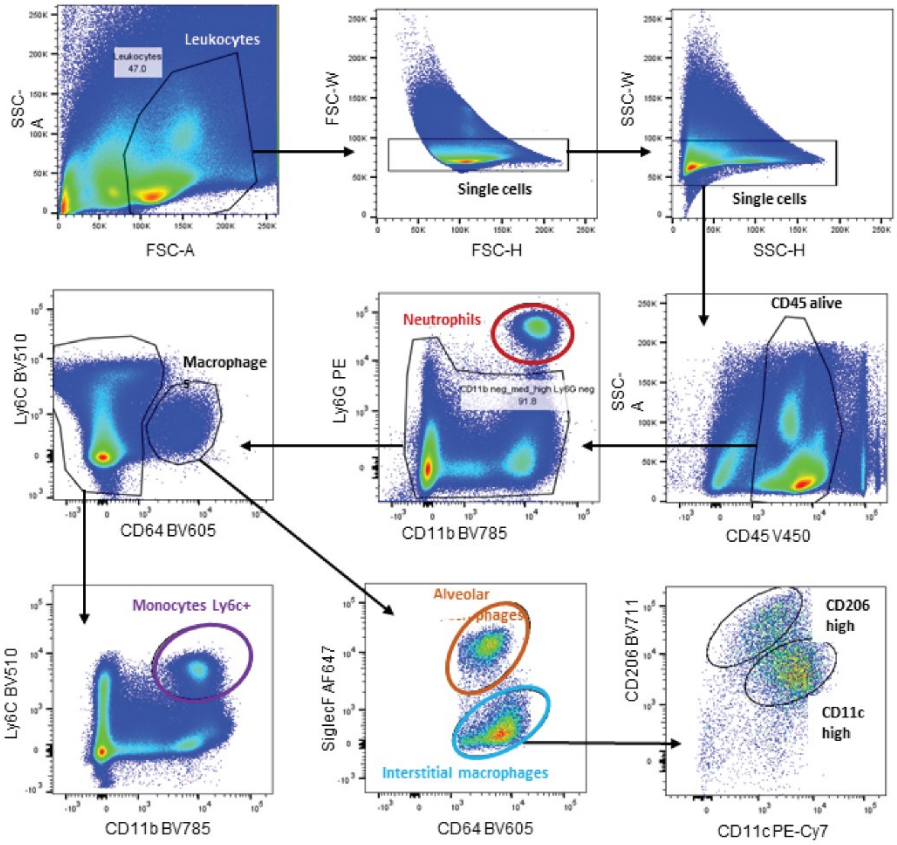

B

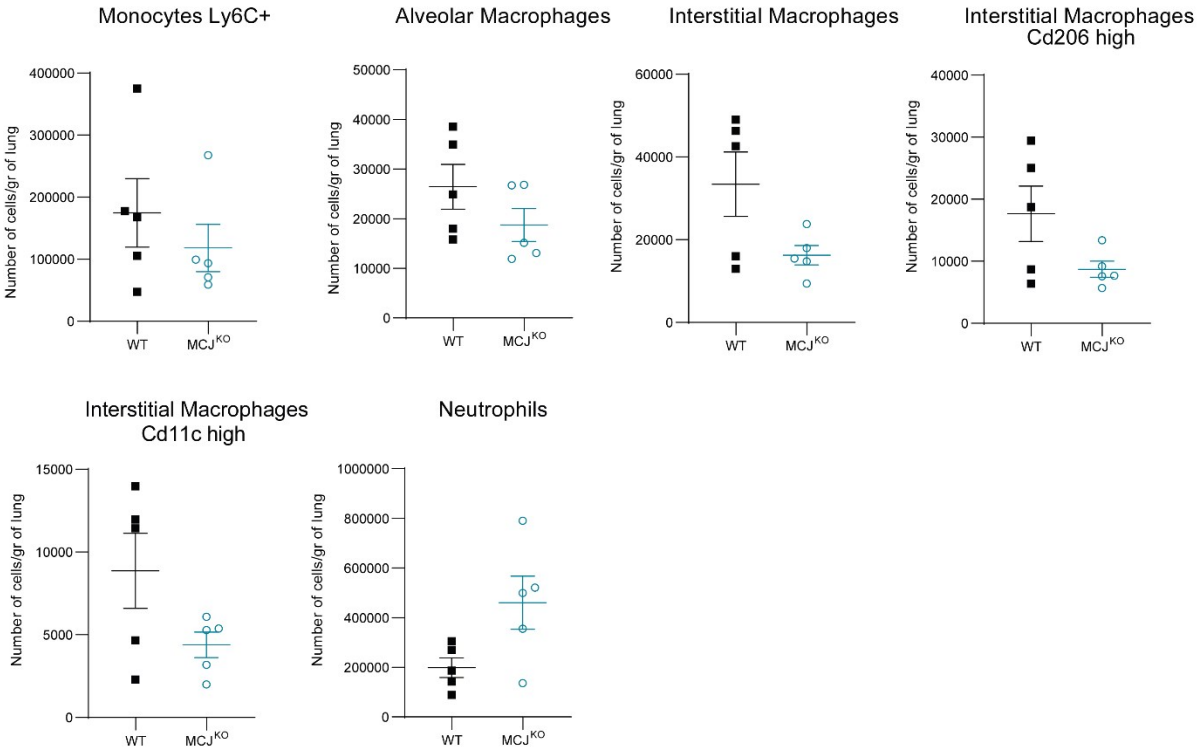

Fig. S3. WT and MCJ^{KO} mice presented no difference in the pulmonary immune cell infiltration and phenotype.

(A) Gating strategy for the analysis of myeloid populations in the stromal vascular fraction. Representative plots are from lungs of normoxic WT mice. Cells were selected based on size and complexity, single cells and viability (DAPI^{-}). Neutrophils (CD45^{+}Ly6G^{+}CD11b^{high}), monocytes (CD11b^{+}Ly6G^{-}Ly6C^{+}) and macrophages (CD11b^{+}Ly6G^{-} Ly6C^{-}CD64^{+}) were analyzed. Within the macrophages population we identified alveolar (SiglecF^{+}CD64^{+}) and interstitial (SiglecF^{-} CD64^{+}) subpopulations. Population of interstitial macrophages was further characterized as two macrophage subtypes: CD11c^{+}CD206^{-} and CD11c^{-}CD206^{+} using the indicated markers. **(B)** The number of immune cells was estimated in the stromal vascular fraction of WT and MCJ^{KO} mice and was normalized by grams of tissue. All data are presented as mean ± s.e.m. Statistical comparison by Student´s t-test (b): NS, *P < 0.05, 67 **P < 0.01, ***P < 0.001.

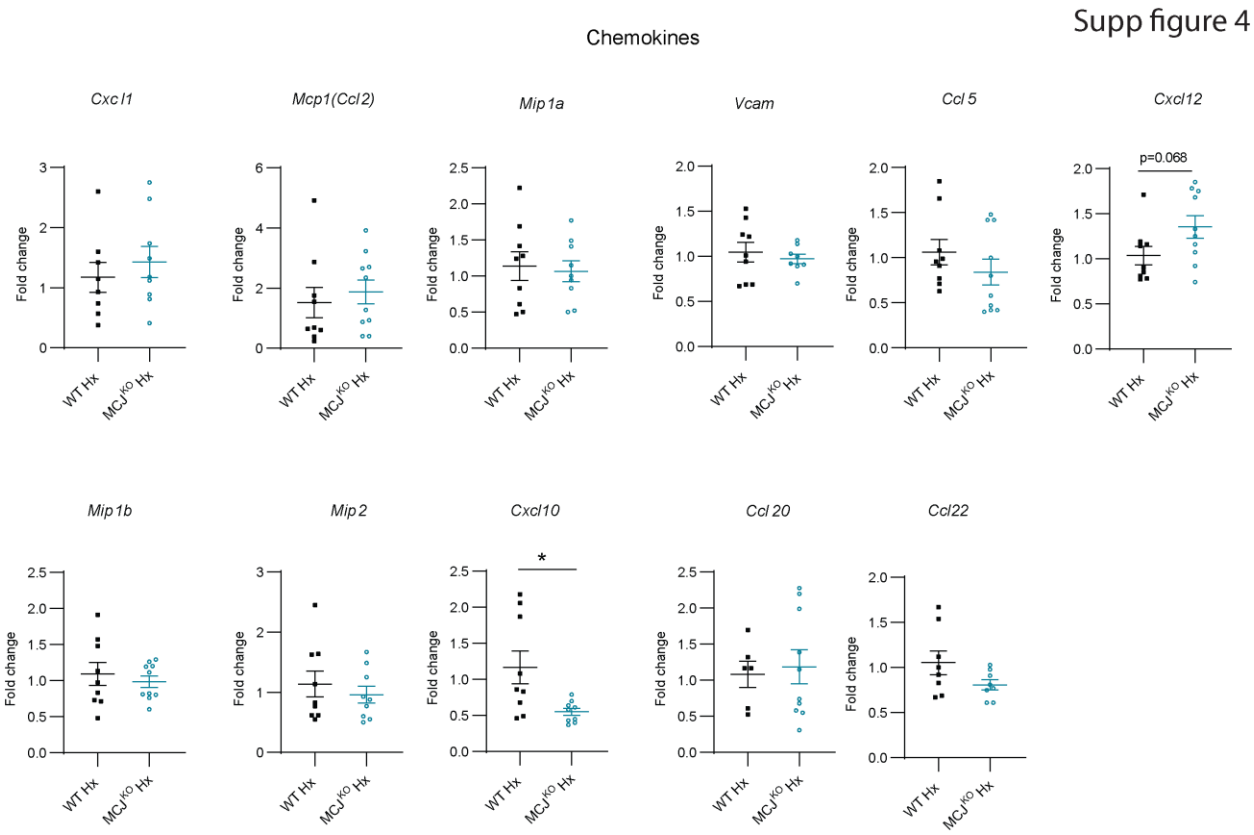

Fig. S4. Lack of MCJ leads to mild alteration of the pulmonary chemokine expression profile after hypoxia.

Lung expression profile of chemokines in WT and MCJ^{KO} mice exposed to hypoxia (Hx, 10% O_2) (n=6-10). All data are presented as mean ± s.e.m. Statistical comparison by student´s t-test: NS (nonsignificant), *P < 0.05, **P < 0.01, ***P < 0.001.

Supp figure 5

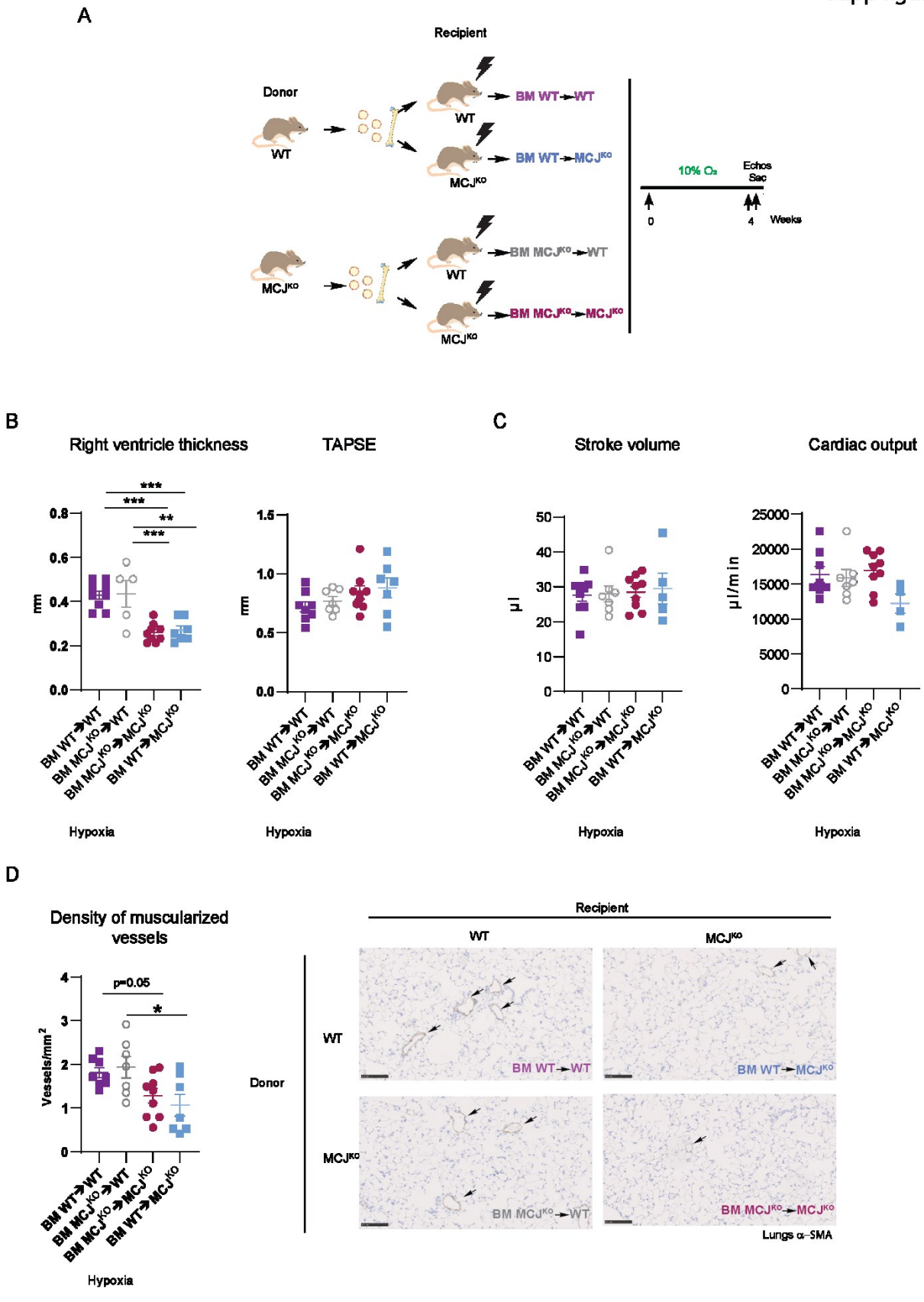

Fig. S5. MCJ^{KO} mice are protected against PH independently of their immune cell population.

(A) WT and MCJ^{KO} mice were irradiated and their bone marrow was reconstituted with donor cells from WT or MCJ^{KO} mice. After reconstitution, mice were exposed to hypoxia for 4 weeks and the cardiac and pulmonary phenotype was evaluated. **(B)** Echocardiography assessment of right ventricle hypertrophy (right ventricle thickness) and function (tricuspid annular plane systolic excursion, TAPSE) in hypoxic mice (n=5-9). **(C)** Echocardiography assessment of stroke volume and cardiac output in hypoxic mice (n=5-9). **(D)** Muscularized vessel density in lungs of mice exposed to hypoxia with a representative immunohistochemistry of α-smooth muscle actin (α-SMA) in hypoxic lungs (n=7-9). Scale bars, 100 μm. All data are presented as mean ± s.e.m. Statistical comparison by one-way ANOVA with Tukey post-test (b,c,d): NS, *P < 0.05, **P < 0.01, ***P < 0.001. Panel A prepared using modified figures from Servier Medical Art (https://smart.servier.com/), licensed under a Creative Commons Attribution 3.0 unported license.

Supp figure 6

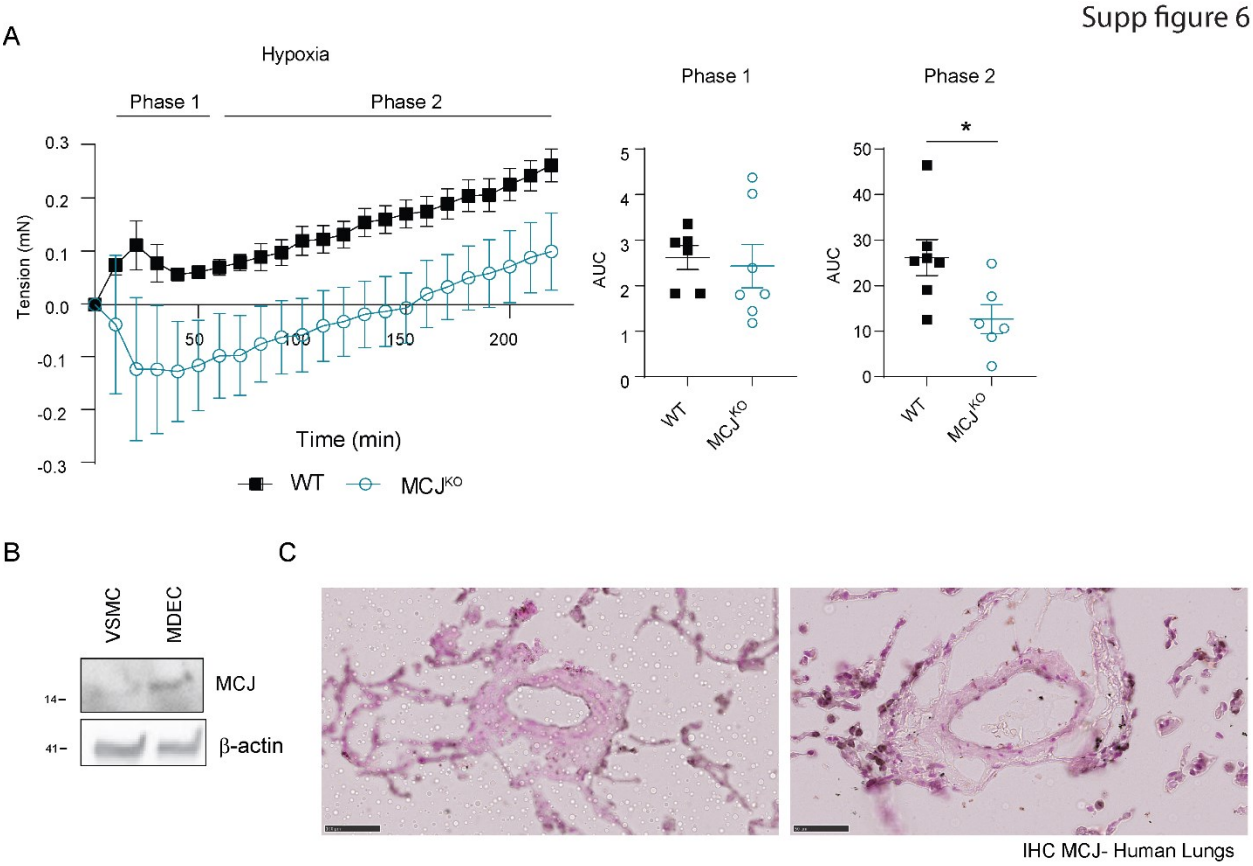

Fig. S6. MCJ contributes to the EC-dependent sustained phase of hypoxic vasoconstriction.

(A) Contractile responses of isolated pulmonary arteries from WT and MCJ^{KO} mice exposed to acute Hx (1% O_2) (n=6-7). The inset graph shows area under the curve [AUC] for phase 1 and 2 of the myography. **(B)** Immunoblot showing MCJ expression in vascular smooth muscle cells (VSMC) and endothelial cells (EC). **(C)** Immunohistochemistry against MCJ in vessels from human lung samples. Scale bar: 100 µm. All data are presented as mean ± s.e.m. Statistical comparison by two-tailed Student t-test (a): NS, *P < 0.05, **P < 0.01, ***P < 0.001.

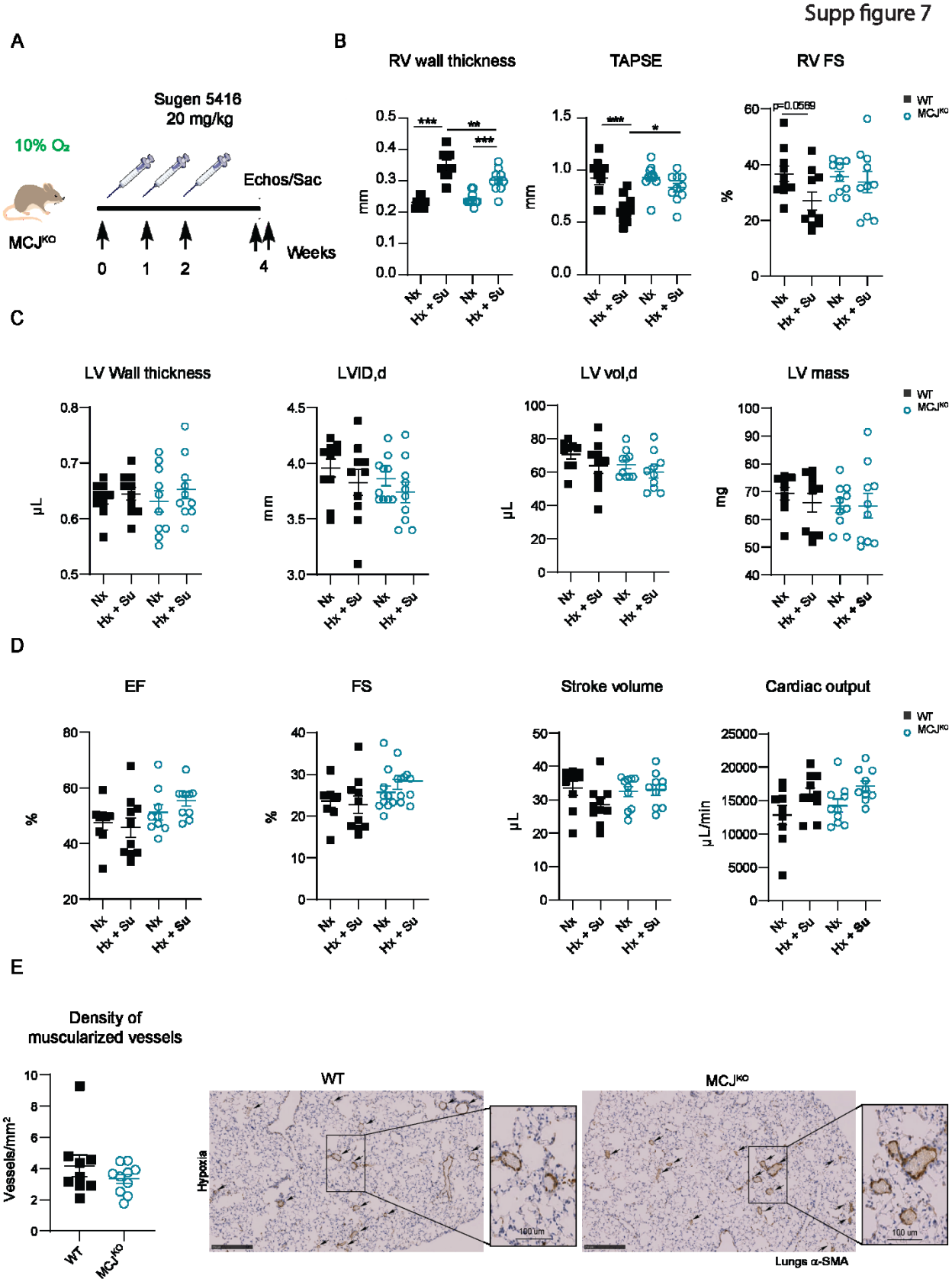

Fig. S7. MCJ deletion conserves cardiac function despite RV hypertrophy and pulmonary

vascular remodeling in a more severe PAH model of hypoxia with Sugen 5416.

(A) Experimental scheme for A-E. WT and MCJ^{KO} mice were i.p. injected at 0,1 and 2 weeks with 20 mg/kg of Sugen 5416 (Su) during chronic hypoxia exposure (Hx, 10% O_2), normoxic mice were kept at normoxia (Nx, 21% O_2) for 4 weeks, and cardiac and pulmonary phenotypes were characterized. **(B)** Echocardiography assessment of right ventricle hypertrophy (right ventricle thickness) and function (tricuspid annular plane systolic excursion, TAPSE and right ventricular fractional shortening, RV FS) (n=9-10). **(C)** Left ventricle characterization (n=9-10). Wall thickness, left ventricular diameter in diastole (LVID,d), left ventricular volume in diastole (LV vol, d) and left ventricular mass (LV mass) were assessed. **(D)** Assessment of left ventricle function (n=9-10). Ejection fraction (EF), fractional shortening (FS), stroke volume and cardiac output were estimated. **(E)** Muscularized vessel density in lungs of mice exposed to hypoxia with a representative immunohistochemistry of α-smooth muscle actin (α-SMA) in hypoxic lungs (n=9-10). Scale bars, 250 μm, 100 μm (vessel). All data are presented as mean ± s.e.m. Statistical comparison by two-tailed Student t-test (e) or two-way ANOVA with Tukey post-test (b,c,d): NS, *P < 0.05, **P < 0.01, ***P < 0.001. Panel A prepared using modified figures from Servier Medical Art (https://smart.servier.com/), licensed under a Creative Commons Attribution 3.0 unported license.

Supp figure 8

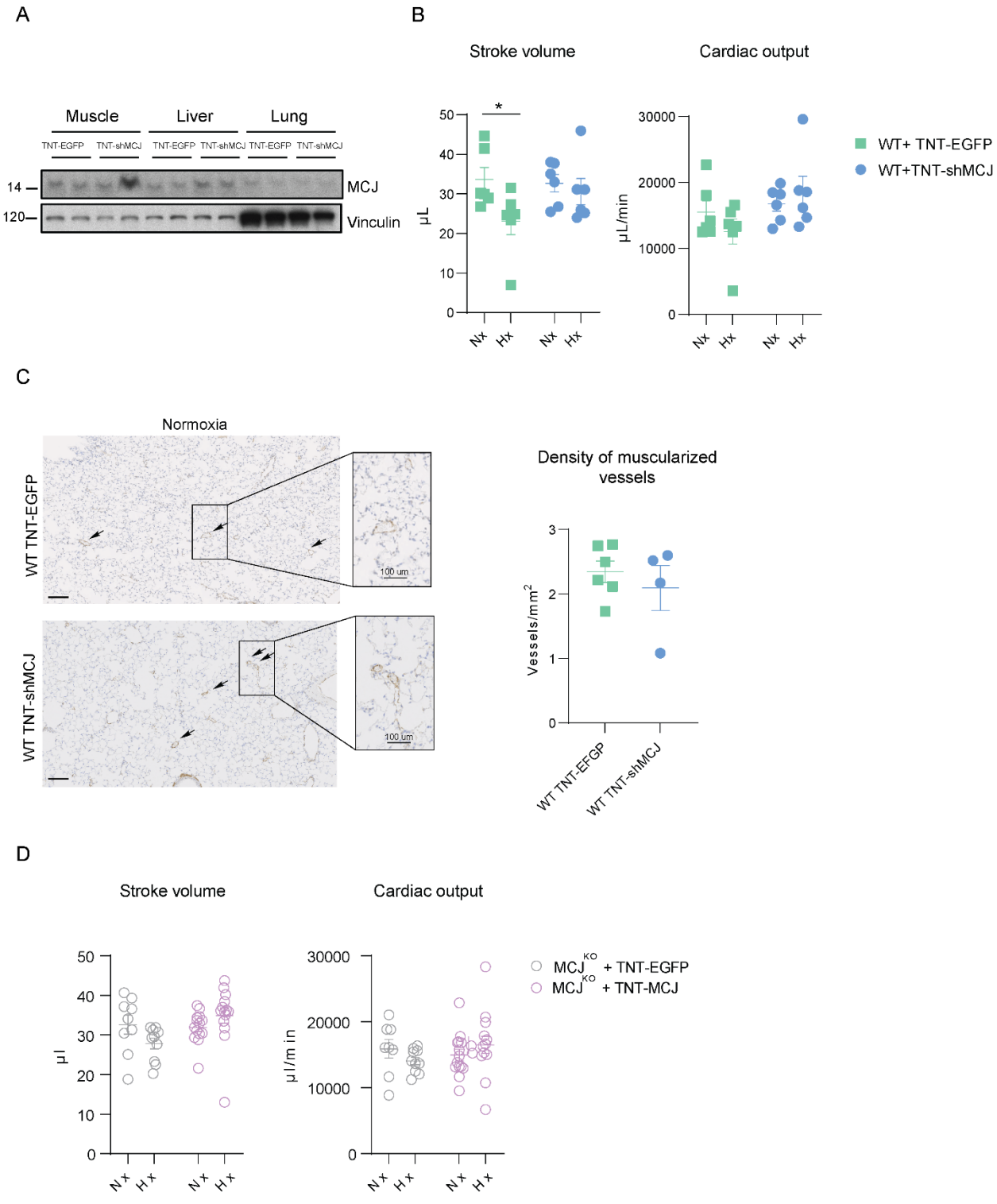

Fig. S8. Effects of cardiac-specific MCJ modulation in normoxia and hypoxia.

(A-C) WT mice were i.v. injected at postnatal day 1 with pAAV-TnT-shMCJ adenovirus to silence specifically MCJ expression in cardiomyocytes (WT TNT-shMCJ) or with control AAV-

TNT-EGFP-Luc (WT TNT-EGFP). Adult mice were maintained in normoxia (Nx, 21% O_2) or exposed to chronic hypoxia (Hx, 10% O_2). **(A)** Immunoblot showing preservation of MCJ expression in muscle, liver, and lung of adult WT mice injected i.v. at postnatal day 1 with the MCJ-targeting adenovirus pAAV-TnT-shMCJ (WT TNT-shMCJ) or the control AAV-TNT-EGFP-Luc (WT TNT-EGFP). **(B)** Echocardiography assessment of stroke volume and cardiac output (n=6). **(C)** Representative immunohistochemistry of α-smooth muscle actin (α-SMA) in normoxic lungs, with amplification of remodelled vessel. Scale bars, 100 μm, 100 μm (vessel). **(D)** MCJ^{KO} mice were i.v. injected at 4 weeks with pAAV-TnT-MCJ adenovirus to achieve cardiomyocyte-specific overexpression of MCJ (MCJ^{KO} TNT-MCJ) or with control AAV-TNT-EGFP-Luc (MCJ^{KO} TNT-EGFP). Adult mice were maintained in normoxia (Nx, 21% O_2) or exposed to chronic hypoxia (Hx, 10% O_2). Echocardiography assessment of stroke volume and cardiac output (n=8-14). All data are presented as mean ± s.e.m. Statistical comparison by Student´s t-test (c) and two-way ANOVA with Tukey post-test (b,d): NS, *P < 0.05, 67 **P < 0.01, ***P < 0.001.

Supp figure 9

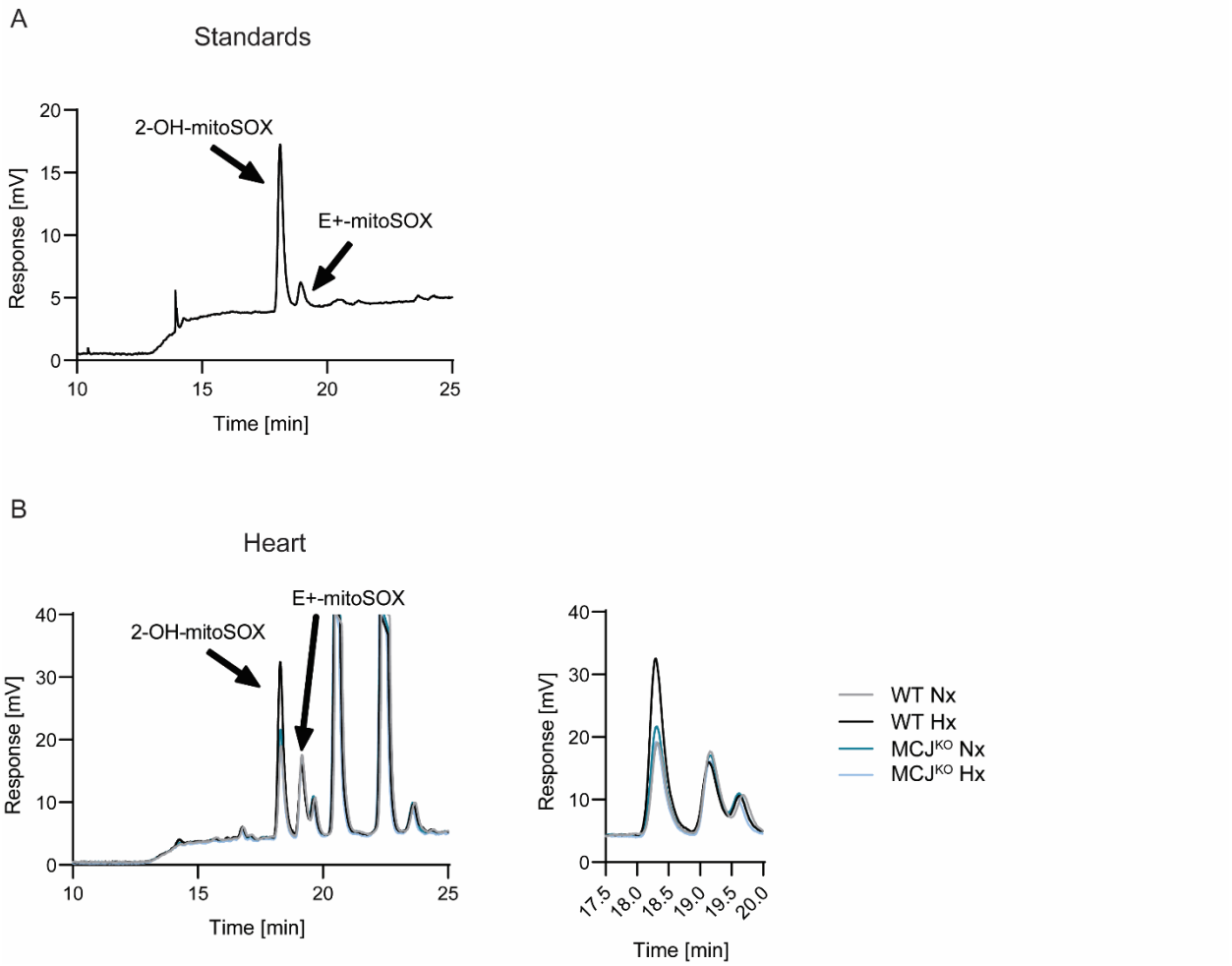

Fig. S9. Detection of superoxide generation by mitoSOX HPLC in isolated cardiac mitochondria.

(A) Representative chromatograms are shown for the 2-OH-mitoSOX and E+mitoSOX standards. **(B)** Representative chromatograms are shown for the HPLC-based quantification of 2-OH-mitoSOX and E+mitoSOX in isolated cardiac mitochondria from normoxic (21% O_2) and hypoxic mice (10% O_2, 7 days). HPLC: high-performance/pressure liquid chromatography; mitoSOX: mitochondria-targeted fluorescence dye triphenylphosphonium-linked hydroethidium.

Supp figure 10

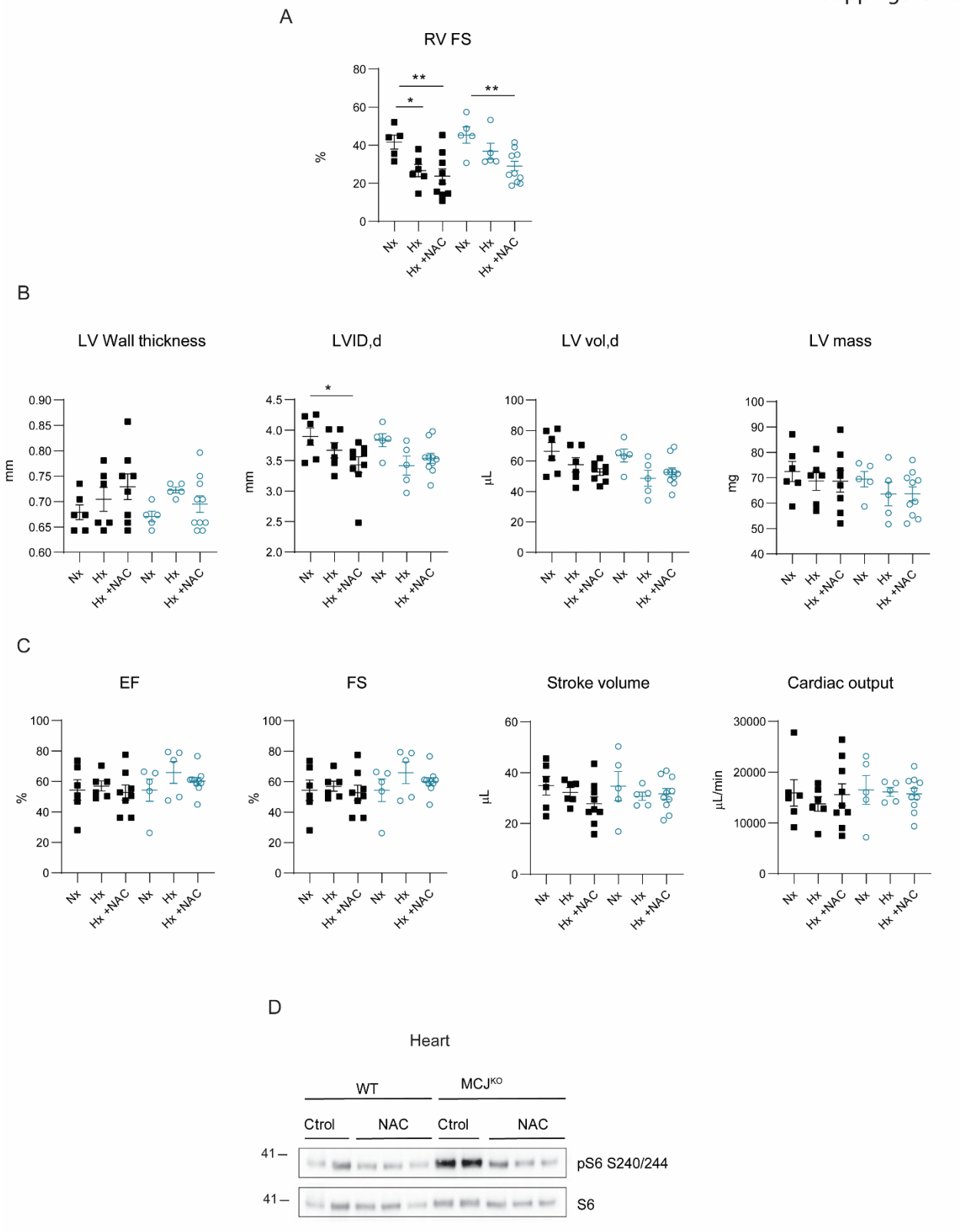

Fig. S10. Mimicking the hypoxic ROS burst in MCJ^{KO} mice leads to RV systolic

dysfunction and LV dilation as in WT hypoxic mice.

(A-C) WT and MCJ^{KO} mice received NAC in drinking water for 2 weeks. After withdrawal of the treatment, they were exposed to chronic hypoxia (Hx, 10% O_2). **(A)** Echocardiography assessment of right ventricle function as RV fractional shortening (n=5-10). **(B)** Left ventricle characterization (n=5-10). Wall thickness, left ventricular diameter in diastole (LVID,d), left ventricular volume in diastole (LV vol, d) and left ventricular mass (LV mass) were measured. **(C)** Assessment of left ventricle function (n=5-10). Ejection fraction (EF), fractional shortening (FS), stroke volume and cardiac output were estimated. **(D)** Mice were i.p. injected during 4 consecutive days with the ROS scavenger N-acetyl-L-cysteine (NAC) and sacrificed at day 5. Representative immunoblots of mTOR pathway activation in normoxic WT and MCJ^{KO} mice injected with NAC or vehicle (control) (n=2-3). Immunoblots for MCJ^{KO} are the ones included in Fig. 4C of the manuscript. Statistical comparison by two-way ANOVA with Tukey´s post-test (a,b,c): NS (non-significant), *P < 0.05, **P < 0.01, ***P < 0.001.

Supp figure 11

A

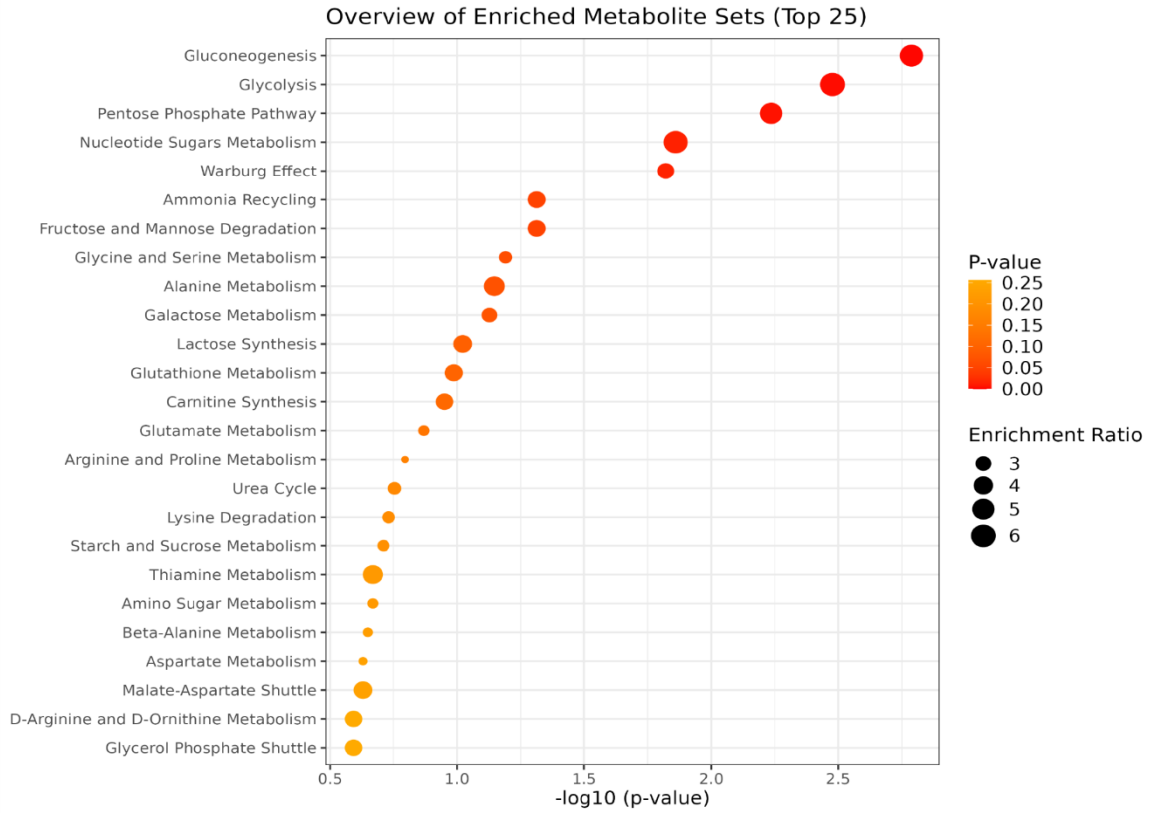

B

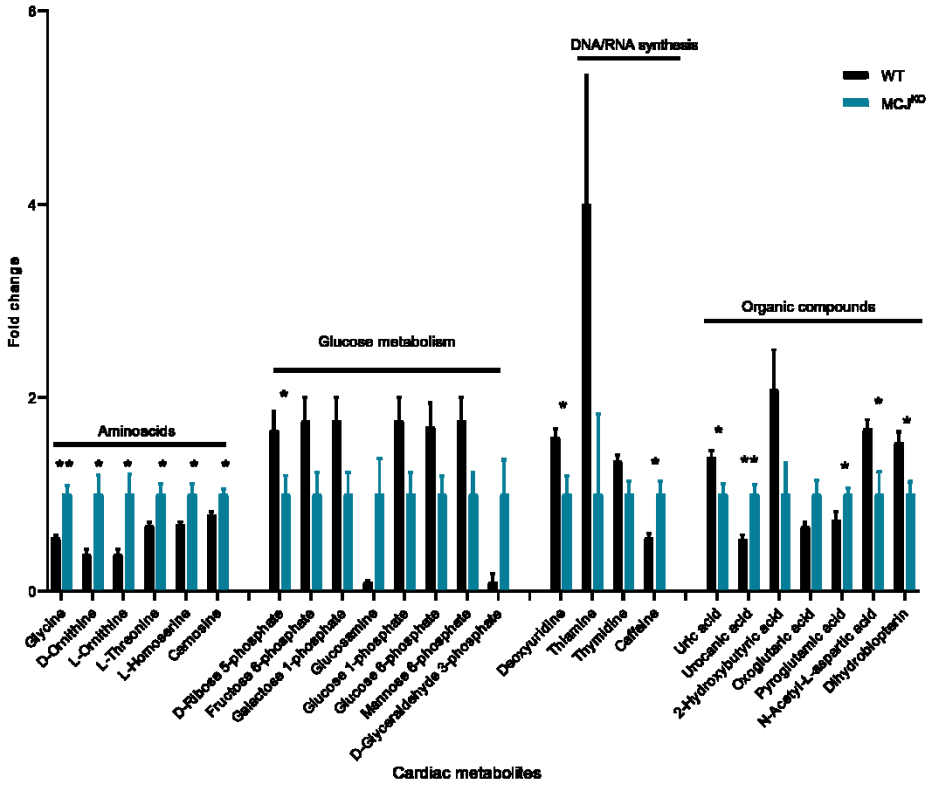

Fig. S11. Metabolic profiling reveals hypoxic metabolite state in MCJ^{KO} hearts.

(A) Pathway enrichment analysis of differential cardiac metabolites in WT and MCJ^{KO} mice using MetaboAnalyst 5.0. In the dot plot chart, the size of the circles per metabolite set represents the Enrichment Ratio and the color represents the p-value (n=4-5). Metabolites differentially encountered are presented in Table S1. **(B)** Relative abundance of the metabolites involved in the pathways in (A) expressed as fold change (MCJ^{KO}= 1). Data regarding the enriched metabolites by pathway is in Table S1. All data are presented as mean ± s.e.m. Statistical comparison by student´s t-test (b): NS (nonsignificant),*P < 0.05, **P < 0.01, ***P < 0.001.

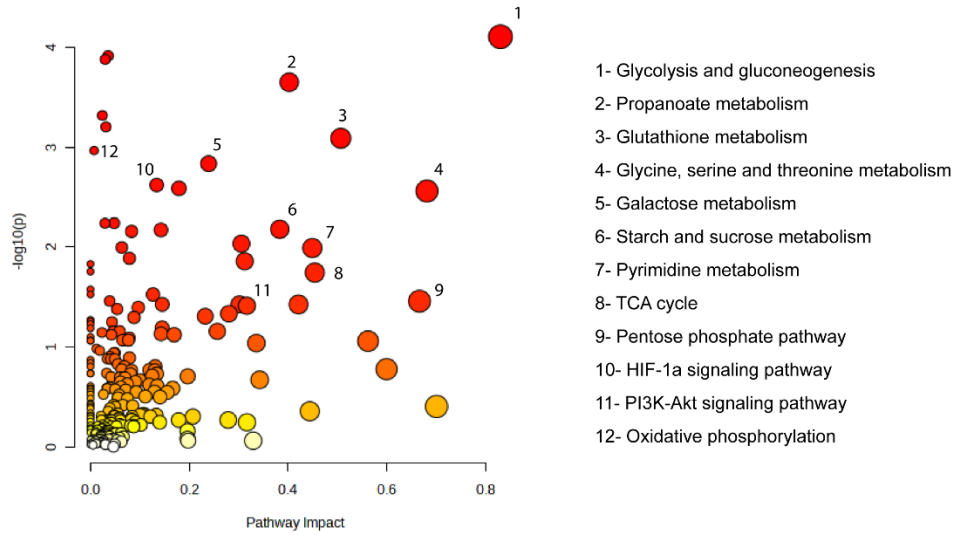

Fig. S12. Cardiac joint pathways analysis.

Integrative analysis of baseline cardiac metabolomics (n=4-5) and proteomics data (n=4) of WT and MCJ^{KO} mice to identify altered pathways using MetaboAnalyst 5.0. The color and size of each circle is based on p-values and pathway impact values. Some of the main identified pathways were indicated with a number and specified on the right. Proteins and metabolites differentially encountered are presented in Table S2. Data integrated using the "all pathways integrated" database, enrichment analysis was performed using the hypergeometric test, degree centrality was used as topology measure and combine query as integration method.

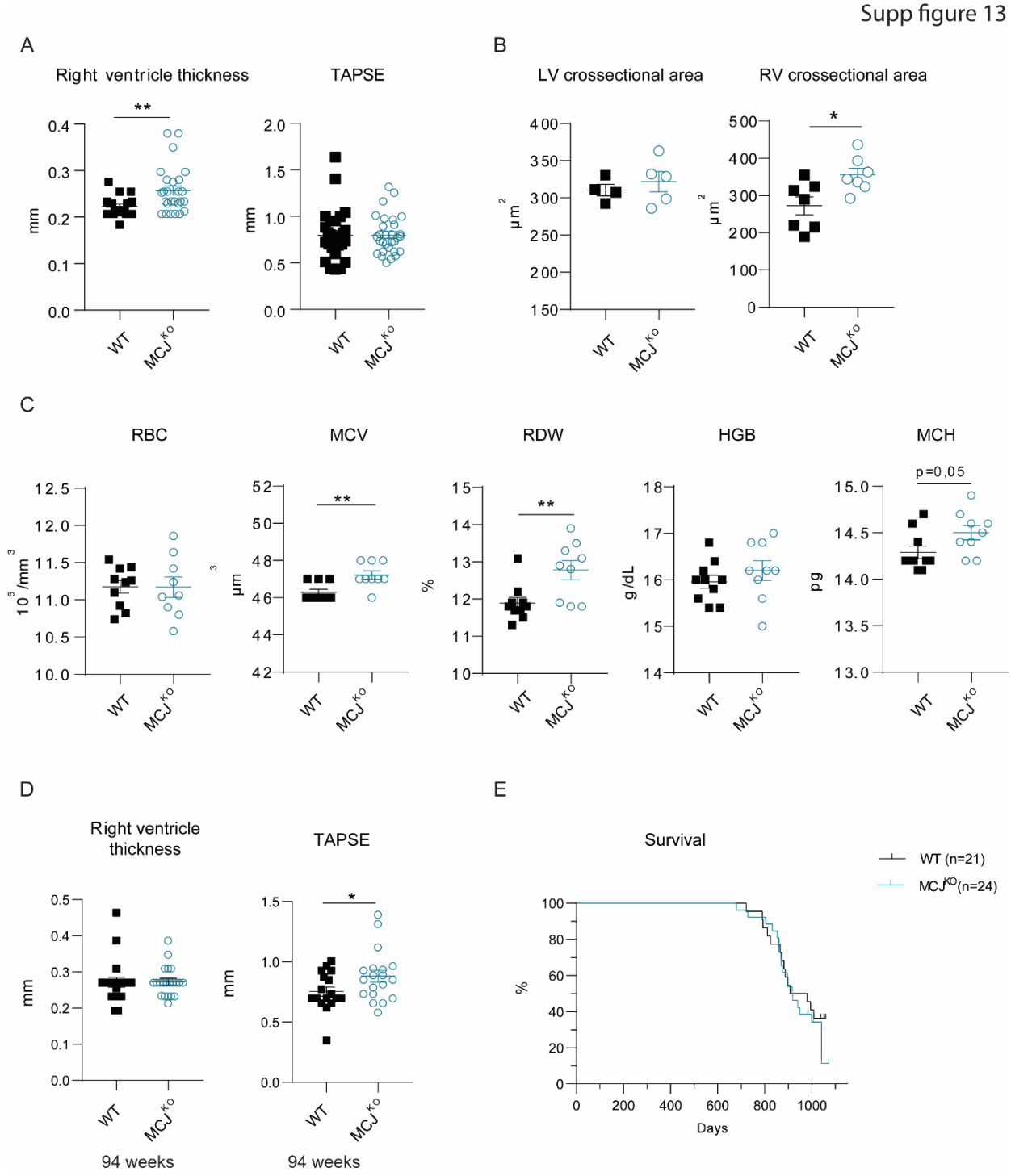

Fig. S13. MCJ depletion leads to alterations in the hematological profile, improved RV function in aged mice and no differences in survival.

(A) The cardiac phenotype of normoxic WT and MCJ^{KO} mice was assessed by echocardiography by measuring the right ventricle hypertrophy (right ventricle thickness) and function (tricuspid annular plane systolic excursion, TAPSE (n=10). **(B)** Cardiomyocyte crossectional area of the

right ventricle (RV) and left ventricle (LV) in normoxic WT and MCJ^{KO} mice measured by WGA immunostaining (n=4-7). **(C)** Hematological analyses in WT and MCJ^{KO} mice: red blood cell (RBC), mean corpuscular volume (MCV), red cell distribution width (RDW), total hemoglobin (HGB) and mean corpuscular hemoglobin (MCH) (n=9-10). **(D)** Echocardiography assessment of right ventricle hypertrophy (right ventricle thickness) and function (tricuspid annular plane systolic excursion, TAPSE) in 94-week-old WT and MCJ^{KO} mice (n=20-21). **(E)** Kaplan-Meier survival curves for WT and MCJ^{KO} mice (n=21-24). All data are presented as mean ± s.e.m. Statistical comparison by two-tailed Student t-test (a,b,c,d) or Mantel-Cox log-rank test (e): NS, *P < 0.05, **P < 0.01, ***P < 0.001.

	Metabolite Set	Total	Hits	Expect	P value	Holm P	FDR	Enriched metabolites
	Gluconeogenesis	35	5	0.923	0.00163	0.16	0.16	fructose 6-phosphate; oxoglutaric acid; D-glyceraldehyde 3-phosphate; glucose 6-phosphate; glucose 1-phosphate
	Glycolysis	25	4	0.659	0.00333	0.323	0.16	fructose 6-phosphate; D-glyceraldehyde 3-phosphate; glucose 6-phosphate; glucose 1-phosphate
	Pentose Phosphate Pathway	29	4	0.765	0.00581	0.557	0.19	fructose 6-phosphate; D-glyceraldehyde 3-phosphate; glucose 6-phosphate; D-ribose 5-phosphate
	Nucleotide Sugars Metabolism	20	3	0.527	0.0138	1	0.3	galactose 1-phosphate; glucose 6-phosphate; glucose 1-phosphate
	Warburg Effect	58	5	1.53	0.0151	1	0.3	fructose 6-phosphate; oxoglutaric acid; D-glyceraldehyde 3-phosphate; glucose 6-phosphate; D-ribose 5-phosphate
	Ammonia Recycling	32	3	0.844	0.0487	1	0.68	glycine; oxoglutaric acid; urocanic acid
	Fructose and Mannose Degradation	32	3	0.844	0.0487	1	0.68	fructose 6-phosphate; mannose 6-phosphate; D-glyceraldehyde 3-phosphate;
	Glycine and Serine Metabolism	59	4	1.56	0.0645	1	0.73	glycine; L-threonine; oxoglutaric acid; ornithine
	Alanine Metabolism	17	2	0.448	0.0714	1	0.73	glycine; oxoglutaric acid
	Galactose Metabolism	38	3	1	0.0746	1	0.73	galactose 1-phosphate; glucose 6-phosphate; glucose 1-phosphate
	Lactose Synthesis	20	2	0.527	0.095	1	0.84	galactose 1-phosphate; glucose 1-phosphate
	Glutathione Metabolism	21	2	0.554	0.103	1	0.84	glycine; pyroglutamic acid;
	Carnitine Synthesis	22	2	0.58	0.112	1	0.84	glycine; oxoglutaric acid
	Glutamate Metabolism	49	3	1.29	0.135	1	0.94	glycine; fructose 6-phosphate; oxoglutaric acid

	Arginine and Proline Metabolism	53	3	1.4	0.16	1	1	glycine; oxoglutaric acid; ornithine
	Urea Cycle	29	2	0.765	0.176	1	1	oxoglutaric acid; ornithine
	Lysine Degradation	30	2	0.791	0.186	1	1	oxoglutaric acid; aminoadipic acid
	Starch and Sucrose Metabolism	31	2	0.817	0.195	1	1	glucose 6-phosphate; glucose 1-phosphate
	Thiamine Metabolism	9	1	0.237	0.215	1	1	thiamine
	Amino Sugar Metabolism	33	2	0.87	0.215	1	1	fructose 6-phosphate; glucosamine
	Beta-Alanine Metabolism	34	2	0.896	0.225	1	1	carnosine; oxoglutaric acid
	Aspartate Metabolism	35	2	0.923	0.235	1	1	oxoglutaric acid; N-acetyl-L-aspartic acid
	Malate-Aspartate Shuttle	10	1	0.264	0.235	1	1	oxoglutaric acid
	D-Arginine and D-Ornithine Metabolism	11	1	0.29	0.256	1	1	D-ornithine
	Glycerol Phosphate Shuttle	11	1	0.29	0.256	1	1	D-glyceraldehyde 3-phosphate
	Glucose-Alanine Cycle	13	1	0.343	0.295	1	1	oxoglutaric acid
	Propanoate Metabolism	42	2	1.11	0.305	1	1	2-hydroxybutyric acid; oxoglutaric acid
	Purine Metabolism	74	3	1.95	0.309	1	1	glycine; uric acid; D-ribose 5-phosphate

	Methionine Metabolism	43	2	1.13	0.315	1	1	glycine; L-homoserine
	Histidine Metabolism	43	2	1.13	0.315	1	1	carnosine; urocanic acid
	Spermidine and Spermine Biosynthesis	18	1	0.475	0.384	1	1	ornithine
	Mitochondrial Electron Transport Chain	19	1	0.501	0.401	1	1	D-glyceraldehyde 3-phosphate
	Catecholamine Biosynthesis	20	1	0.527	0.417	1	1	dihydrobiopterin
	Threonine and 2-Oxobutanoate Degradation	20	1	0.527	0.417	1	1	L-threonine
	Pyrimidine Metabolism	59	2	1.56	0.468	1	1	deoxyuridine; thymidine
	Caffeine Metabolism	24	1	0.633	0.477	1	1	caffeine
	Tryptophan Metabolism	60	2	1.58	0.477	1	1	oxoglutaric acid; 3-hydroxyanthranilic acid
	Cysteine Metabolism	26	1	0.686	0.505	1	1	oxoglutaric acid
	Oxidation of Branched Chain Fatty Acids	26	1	0.686	0.505	1	1	oxoglutaric acid
	Phytanic Acid Peroxisomal Oxidation	26	1	0.686	0.505	1	1	oxoglutaric acid
	Inositol Phosphate Metabolism	26	1	0.686	0.505	1	1	glucose 6-phosphate
	Phenylalanine and Tyrosine Metabolism	28	1	0.738	0.532	1	1	oxoglutaric acid

	Pterine Biosynthesis	29	1	0.765	0.544	1	1	dihydrobiopterin
	Citric Acid Cycle	32	1	0.844	0.58	1	1	oxoglutaric acid
	Inositol Metabolism	33	1	0.87	0.592	1	1	glucose 6-phosphate
	Porphyrin Metabolism	40	1	1.05	0.664	1	1	glycine
	Valine, Leucine and Isoleucine Degradation	60	1	1.58	0.808	1	1	oxoglutaric acid
	Bile Acid Biosynthesis	65	1	1.71	0.834	1	1	glycine
	Tyrosine Metabolism	72	1	1.9	0.864	1	1	oxoglutaric acid

Table S1.

Cardiac metabolomics.

Differentially encountered metabolites ($p<0.05$) were analyzed by Metabolite Set Enrichment Analysis (MSEA) using Metaboanalyst 5.0. The table display the enriched metabolites by pathway.

Pathways	Total	Hits	Expect	Holm adjust	FDR	Proteins and metabolites
Glycolysis or Gluconeogenesis	97	7	1.037	0.026	0.014	L-lactate dehydrogenase B, L-lactate dehydrogenase C, bisphosphoglycerate mutase, phosphoglucomutase 2, phosphoglycerate kinase 2, D-glucose 1-phosphate, glyceraldehyde 3-phosphate
Central carbon metabolism in cancer	104	7	1.112	0.040	0.014	glucose 6-phosphate; 2-oxoglutarate; L-lactate dehydrogenase B; L-lactate dehydrogenase C; Akt; D-fructose 6-phosphate; glycine
Alzheimer disease	180	9	1.924	0.043	0.014	NADH:ubiquinone oxidoreductase core subunit S5; NADH:ubiquinone oxidoreductase subunit A3; NADH:ubiquinone oxidoreductase subunit B8; succinate dehydrogenase complex; ubiquinol cytochrome c reductase core protein 2; SERCA1; SERCA2; apo-E; lpl
Propanoate metabolism	81	6	0.866	0.073	0.018	acetyl-CoA carboxylase; L-lactate dehydrogenase B; L-lactate dehydrogenase C; 2-hydroxybutyric acid; succinate-Coenzyme A ligase; dihydrolipoyl transacylase
Glucagon signaling pathway	130	7	1.390	0.156	0.032	2-oxoglutarate; D-fructose 6-phosphate; D-glucose 1-phosphate; Akt; acetyl-CoA carboxylase; L-lactate dehydrogenase B; L-lactate dehydrogenase C
Prion diseases	37	4	0.396	0.202	0.034	laminin; tyrosine-protein kinase Fyn; complement component 7; complement component 5
Glutathione metabolism	103	6	1.101	0.261	0.038	glutathione peroxidase 4; glutathione S-transferase; pyroglutamic acid; glycine; glutathione reductase; ornithine
Oxidative phosphorylation	149	7	1.593	0.346	0.044	NADH:ubiquinone oxidoreductase subunit B8; NADH:ubiquinone oxidoreductase subunit A3; NADH:ubiquinone oxidoreductase core subunit S5; cytochrome c oxidase assembly protein 15; ubiquinol cytochrome c reductase core protein 2; ATP synthase membrane subunit f; succinate dehydrogenase complex
Galactose metabolism	78	5	0.834	0.466	0.053	phosphoglucomutase 2; D-glucose 1-phosphate; alpha-D-galactose 1-phosphate; glyceraldehyde 3-phosphate; D-Fructose 6-phosphate
HIF-1 signaling pathway	127	6	1.358	0.761	0.075	Akt; L-lactate dehydrogenase B; L-lactate dehydrogenase C; phosphoglycerate kinase 2; 2-oxoglutarate; eIF-4E
Thyroid hormone signaling pathway	129	6	1.379	0.820	0.075	Akt; phospholipase C; SERCA1; SERCA2; phospholamban; Notch2
Glycine, serine and threonine metabolism	90	5	0.962	0.869	0.075	threonine aldolase 1; glycine; L-threonine; L-homoserine; bisphosphoglycerate mutase
Thermogenesis	253	8	2.705	1	0.134	cGMP-dependent protein kinase 1; cytochrome c oxidase assembly protein 15; NADH:ubiquinone oxidoreductase core subunit S5; NADH:ubiquinone oxidoreductase subunit A3; succinate dehydrogenase complex; ubiquinol cytochrome c reductase core protein 2; NADH:ubiquinone oxidoreductase subunit B8; ATP synthase membrane subunit f
Non-alcoholic fatty liver disease (NAFLD)	152	6	1.625	1	0.134	Akt; NADH:ubiquinone oxidoreductase core subunit S5; NADH:ubiquinone oxidoreductase subunit A3; NADH:ubiquinone oxidoreductase subunit B8; succinate dehydrogenase complex; ubiquinol cytochrome c reductase core protein 2
Starch and sucrose metabolism	70	4	0.748	1	0.134	glucose 6-phosphate; phosphoglucomutase 2; D-fructose 6-phosphate; D-glucose 1-phosphate
Amino sugar and nucleotide sugar metabolism	157	6	1.678	1	0.134	D-glucosamine; phosphoglucomutase 2; alpha-D-galactose 1-phosphate; D-glucose 1-phosphate; D-mannose 6-phosphate; D-xylose
D-Arginine and D-ornithine metabolism	12	2	0.128	1	0.134	ornithine; D-ornithine
Inositol phosphate metabolism	120	5	1.283	1	0.167	myo-inositol-1-phosphate synthase; phospholipase C; glucose 6-phosphate; glyceraldehyde 3-phosphate; phosphatidylinositol 4-phosphatase
Arrhythmogenic right ventricular cardiomyopathy (ARVC)	79	4	0.845	1	0.167	SERCA1; SERCA2; desmoglein 2; desmoplakin

Pyrimidine metabolism	123	5	1.315	1	0.167	nucleoside diphosphate kinase 1; L-dihydroorotate; thymidine; malonate; deoxyuridine
Thiamine metabolism	46	3	0.492	1	0.202	glyceraldehyde 3-phosphate; thiamine; glycine
D-Glutamine and D-glutamate metabolism	17	2	0.182	1	0.206	D-glutamate cyclase; 2-oxoglutarate
ABC transporters	186	6	1.988	1	0.210	D-xylose; ornithine; L-threonine; thiamine; glycine; deoxyuridine
Protein digestion and absorption	141	5	1.507	1	0.236	glycine; L-Threonine; collagen type XVIII; collagen type VI alpha; collagen type XXIV
Citrate cycle (TCA cycle)	52	3	0.556	1	0.236	succinate-Coenzyme A ligase; 2-oxoglutarate; succinate dehydrogenase complex
Parkinson disease	157	5	1.678	1	0.334	NADH:ubiquinone oxidoreductase core subunit S5; NADH:ubiquinone oxidoreductase subunit A3; NADH:ubiquinone oxidoreductase subunit B8; succinate dehydrogenase complex; ubiquinol cytochrome c reductase core protein 2
Phosphonate and phosphinate metabolism	63	3	0.673	1	0.349	phosphonoacetic acid; ribose 5-phosphate;glycine
Adrenergic signaling in cardiomyocytes	162	5	1.732	1	0.349	SERCA1; SERCA2; Akt; phospholamban; protein phosphatase 2
Lysine degradation	115	4	1.229	1	0.372	glutaric acid; L-2-aminoadipic acid; glycine; 2-oxoglutarate
Pentose phosphate pathway	67	3	0.716	1	0.372	phosphoglucomutase 2; glyceraldehyde 3-phosphate; ribose 5-phosphate
Butanoate metabolism	69	3	0.738	1	0.372	3-hydroxybutyrate dehydrogenase; maleate; 2-oxoglutarate
Pyruvate metabolism	69	3	0.738	1	0.372	L-lactate dehydrogenase B; L-lactate dehydrogenase C; acetyl-CoA carboxylase
Purine metabolism	231	6	2.470	1	0.372	nucleoside diphosphate kinase 1; guanine deaminase; phosphoglucomutase 2; ribose 5-phosphate; uric acid; glycine
PI3K-Akt signaling pathway	359	8	3.838	1	0.372	eIF-4E; Akt; 14-3-3 protein epsilon ; thioesterase superfamily member 4; protein phosphatase 2 ; laminin B1; laminin; collagen type VI alpha
Histidine metabolism	71	3	0.759	1	0.377	carnosine; urocanate; 2-oxoglutarate
Ferroptosis	72	3	0.770	1	0.379	glutathione peroxidase 4; ferritin heavy chain ; lysophosphatidylcholine acyltransferase 3
cGMP-PKG signaling pathway	183	5	1.956	1	0.411	cGMP-dependent protein kinase 1; SERCA1; SERCA2; phospholamban; Akt
Fatty acid biosynthesis	77	3	0.823	1	0.424	acetyl-CoA carboxylase ; malonate; 7 beta-estradiol 17-dehydrogenase
Insulin resistance	130	4	1.390	1	0.425	Akt; acetyl-CoA carboxylase; glucose 6-phosphate; D-fructose 6-phosphate
Collecting duct acid secretion	35	2	0.374	1	0.439	solute carrier family 4 ; carbonic anhydrase 2

Mineral absorption	81	3	0.866	1	0.439	ferritin heavy chain; glycine; L-threonine
Nitrogen metabolism	36	2	0.385	1	0.439	carbonic anhydrase 1; carbonic anhydrase 2
Huntington disease	196	5	2.095	1	0.450	NADH:ubiquinone oxidoreductase core subunit S5; NADH:ubiquinone oxidoreductase subunit A3; NADH:ubiquinone oxidoreductase subunit B8; succinate dehydrogenase complex; ubiquinol cytochrome c reductase core protein 2
Focal adhesion	201	5	2.149	1	0.472	Akt; tyrosine-protein kinase Fyn; laminin B1; laminin; collagen type VI alpha
Proximal tubule bicarbonate reclamation	39	2	0.417	1	0.472	carbonic anhydrase 2; 2-oxoglutarate
Complement and coagulation cascades	89	3	0.951	1	0.475	serine (or cysteine) peptidase inhibitor; complement component 5; complement component 7
Pentose and glucuronate interconversions	89	3	0.951	1	0.475	D-glucose 1-phosphate; D-xylose; 2-oxoglutarate
ECM-receptor interaction	89	3	0.951	1	0.475	laminin B1; laminin; collagen type VI alpha
Cardiac muscle contraction	90	3	0.962	1	0.475	SERCA1; SERCA2; ubiquinol cytochrome c reductase core protein 2
Arginine biosynthesis	42	2	0.449	1	0.475	ornithine; 2-oxoglutarate
AMPK signaling pathway	149	4	1.593	1	0.475	Akt; D-fructose 6-phosphate; acetyl-CoA carboxylase ; protein phosphatase 2
PPAR signaling pathway	92	3	0.984	1	0.475	perilipin-2 ; acyl-CoA dehydrogenase; Lpl
Thyroid hormone synthesis	94	3	1.005	1	0.485	glucose 6-phosphate; ribose 5-phosphate; glutathione reductase
Small cell lung cancer	95	3	1.016	1	0.485	Akt; laminin B1; laminin
Dilated cardiomyopathy (DCM)	97	3	1.037	1	0.485	SERCA1; SERCA2; phospholamban
Gap junction	97	3	1.037	1	0.485	cGMP-dependent protein kinase 1; tubulin beta 2; tubulin beta 4
Proteasome	46	2	0.492	1	0.485	proteasome activator subunit 1; 20S proteasome subunit alpha 6
African trypanosomiasis	46	2	0.492	1	0.485	hemoglobin subunit beta; hemoglobin subunit alpha
Valine, leucine and isoleucine degradation	98	3	1.048	1	0.485	acyl-Coenzyme A dehydrogenase; dihydrolipoyl transacylase; acyl-CoA dehydrogenase
Fatty acid degradation	100	3	1.069	1	0.500	acyl-Coenzyme A dehydrogenase; acyl-CoA dehydrogenase; glutaric acid
Retrograde endocannabinoid signaling	167	4	1.785	1	0.557	solute carrier family 32 ; NADH:ubiquinone oxidoreductase core subunit S5; NADH:ubiquinone oxidoreductase subunit A3; NADH:ubiquinone oxidoreductase subunit B8

Protein processing in endoplasmic reticulum	170	4	1.817	1	0.575	protein kinase C substrate 80K-H ; translocation protein SEC63;DnaJ homolog subfamily A member 1; protein transport protein SEC31
cAMP signaling pathway	240	5	2.566	1	0.592	SERCA1; SERCA2; Akt; phospholamban; phospholipase C
Toxoplasmosis	111	3	1.187	1	0.592	Akt; laminin B1; laminin
Cysteine and methionine metabolism	115	3	1.229	1	0.629	L-lactate dehydrogenase B; L-lactate dehydrogenase C; L-homoserine
Phagosome	181	4	1.935	1	0.629	rab-interacting lysosomal protein; tubulin beta; tubulin beta 4; lysosomal-associated membrane protein 2
Cholesterol metabolism	59	2	0.631	1	0.629	apo-E; lpl
Aminoacyl-tRNA biosynthesis	118	3	1.262	1	0.629	isoleucyl-tRNA synthetase 1; L-threonine; glycine
Porphyrin and chlorophyll metabolism	183	4	1.956	1	0.629	glycine; biliverdin reductase B; cytochrome c oxidase assembly protein 15; L-threonine
Malaria	60	2	0.641	1	0.629	hemoglobin subunit beta; hemoglobin subunit alpha
Pancreatic secretion	123	3	1.315	1	0.666	carbonic anhydrase 2; SERCA1; SERCA2
beta-Alanine metabolism	64	2	0.684	1	0.679	malonate; carnosine
Alanine, aspartate and glutamate metabolism	66	2	0.706	1	0.686	2-oxoglutarate; N-acetyl-L-aspartate
Lysosome	128	3	1.368	1	0.686	palmitoyl-protein thioesterase 1; lysosomal-associated membrane protein 2; D-mannose 6-phosphate
Arginine and proline metabolism	128	3	1.368	1	0.686	creatine kinase; ornithine; 4-guanidinobutanoate
Synthesis and degradation of ketone bodies	17	1	0.182	1	0.703	3-hydroxybutyrate dehydrogenase
Fatty acid elongation	69	2	0.738	1	0.703	palmitoyl-protein thioesterase 1; thioesterase superfamily member 4
Calcium signaling pathway	202	4	2.159	1	0.703	phospholipase C; SERCA1; SERCA2; phospholamban
Regulation of lipolysis in adipocytes	70	2	0.748	1	0.703	cGMP-dependent protein kinase 1; Akt
Long-term depression	70	2	0.748	1	0.703	cGMP-dependent protein kinase 1; protein phosphatase 2
Bacterial invasion of epithelial cells	73	2	0.780	1	0.716	septin 8; septin 11
Carbohydrate digestion and absorption	73	2	0.780	1	0.716	glucose 6-phosphate; Akt

Sulfur relay system	19	1	0.203	1	0.716	thiamine
Platelet activation	139	3	1.486	1	0.716	Akt; cGMP-dependent protein kinase 1; tyrosine-protein kinase Fyn
Sphingolipid signaling pathway	139	3	1.486	1	0.716	Akt; protein phosphatase 2 ; tyrosine-protein kinase Fyn
Human papillomavirus infection	364	6	3.891	1	0.737	Akt; laminin B1; laminin; collagen type VI alpha; Notch2; protein phosphatase 2
Insulin signaling pathway	143	3	1.529	1	0.737	acetyl-CoA carboxylase ; eIF-4E; Akt
Autophagy - animal	144	3	1.539	1	0.737	Akt; protein phosphatase 2 ; lysosomal-associated membrane protein 2
Fc epsilon RI signaling pathway	78	2	0.834	1	0.737	tyrosine-protein kinase Fyn; Akt
Adipocytokine signaling pathway	78	2	0.834	1	0.737	acetyl-CoA carboxylase ; Akt
Glycerophospholipid metabolism	149	3	1.593	1	0.763	diethanolamine; lysophosphatidylcholine acyltransferase 3; phospholipase A2
Platinum drug resistance	81	2	0.866	1	0.763	glutathione S-transferase; Akt
Prolactin signaling pathway	83	2	0.887	1	0.774	Akt; glucose 6-phosphate
EGFR tyrosine kinase inhibitor resistance	83	2	0.887	1	0.774	Akt; eIF-4E
Pertussis	86	2	0.919	1	0.807	serine (or cysteine) peptidase inhibitor; complement component 5
mTOR signaling pathway	158	3	1.689	1	0.814	Akt; eIF-4E; MAPK and MTOR activator 2
Synaptic vesicle cycle	89	2	0.951	1	0.821	glycine; solute carrier family 32
Fructose and mannose metabolism	89	2	0.951	1	0.821	D-mannose 6-phosphate; glyceraldehyde 3-phosphate
Hepatitis C	162	3	1.732	1	0.821	protein phosphatase 2 ; Akt; 14-3-3 protein epsilon
Valine, leucine and isoleucine biosynthesis	27	1	0.289	1	0.821	L-threonine
Protein export	28	1	0.299	1	0.821	translocation protein SEC63
Caffeine metabolism	28	1	0.299	1	0.821	caffeine
Riboflavin metabolism	28	1	0.299	1	0.821	biliverdin reductase B

Glyoxylate and dicarboxylate metabolism	93	2	0.994	1	0.821	2-oxoglutarate; glycine
Hypertrophic cardiomyopathy (HCM)	94	2	1.005	1	0.821	SERCA1; SERCA2
Progesterone-mediated oocyte maturation	94	2	1.005	1	0.821	Akt; serine/threonine kinase 10
mRNA surveillance pathway	95	2	1.016	1	0.825	protein phosphatase 2 ; DAZ associated protein 1
GABAergic synapse	98	2	1.048	1	0.838	solute carrier family 32; 2-oxoglutarate
Fc gamma R-mediated phagocytosis	98	2	1.048	1	0.838	Akt; phospholipase A2
Longevity regulating pathway	98	2	1.048	1	0.838	Akt; eIF-4E
Glycerolipid metabolism	99	2	1.058	1	0.842	Lpl; D-glucose 1-phosphate
Taurine and hypotaurine metabolism	33	1	0.353	1	0.865	2-oxoglutarate
SNARE interactions in vesicular transport	33	1	0.353	1	0.865	syntaxin 8
Endocrine resistance	103	2	1.101	1	0.865	Akt; notch2
Autophagy - other	35	1	0.374	1	0.893	protein phosphatase 2
T cell receptor signaling pathway	107	2	1.144	1	0.895	Akt; tyrosine-protein kinase Fyn
Chagas disease (American trypanosomiasis)	108	2	1.155	1	0.898	Akt; protein phosphatase 2
Vitamin B6 metabolism	37	1	0.396	1	0.905	glyceraldehyde 3-phosphate
AGE-RAGE signaling pathway in diabetic complications	110	2	1.176	1	0.905	Akt; phospholipase C
Amoebiasis	120	2	1.283	1	1	laminin B1; laminin
Sulfur metabolism	44	1	0.470	1	1	L-homoserine
Oocyte meiosis	123	2	1.315	1	1	14-3-3 protein epsilon ; protein phosphatase 2
Cholinergic synapse	124	2	1.326	1	1	Akt; tyrosine-protein kinase Fyn
Neurotrophin signaling pathway	126	2	1.347	1	1	Akt; 14-3-3 protein epsilon

Phosphatidylinositol signaling system	127	2	1.358	1	1	phospholipase C; phosphatidylinositol 4-phosphatase
Proteoglycans in cancer	212	3	2.266	1	1	ankyrin; Akt; phospholipase C
Nicotine addiction	47	1	0.502	1	1	solute carrier family 32
Osteoclast differentiation	131	2	1.400	1	1	tyrosine-protein kinase Fyn; Akt
Spliceosome	132	2	1.411	1	1	splicing factor 3A subunit 3 ; heterogeneous nuclear ribonucleoprotein C1/C2
Notch signaling pathway	54	1	0.577	1	1	nNotch2
Apoptosis	140	2	1.497	1	1	Akt; spectrin alpha chain
Systemic lupus erythematosus	145	2	1.550	1	1	complement component 5; complement component 7
Dopaminergic synapse	146	2	1.561	1	1	Akt; protein phosphatase 2
Endometrial cancer	59	1	0.631	1	1	Akt
Ras signaling pathway	239	3	2.555	1	1	Akt; phospholipase C; phospholipase A2
Breast cancer	150	2	1.604	1	1	notch2; Akt
Drug metabolism - other enzymes	151	2	1.614	1	1	nucleoside diphosphate kinase 1;glutathione S-transferase
Fluid shear stress and atherosclerosis	152	2	1.625	1	1	Akt; glutathione S-transferase
Bile secretion	246	3	2.630	1	1	carbonic anhydrase 2; uric acid; 2-oxoglutarate
Hippo signaling pathway	154	2	1.646	1	1	14-3-3 protein epsilon ; protein phosphatase 2
Vitamin digestion and absorption	63	1	0.673	1	1	thiamine
Primary bile acid biosynthesis	63	1	0.673	1	1	glycine
VEGF signaling pathway	64	1	0.684	1	1	Akt
Longevity regulating pathway - multiple species	64	1	0.684	1	1	Akt
Vascular smooth muscle contraction	156	2	1.668	1	1	phospholipase A2; cGMP-dependent protein kinase 1

Phospholipase D signaling pathway	159	2	1.700	1	1	Akt; tyrosine-protein kinase Fyn
Terpenoid backbone biosynthesis	68	1	0.727	1	1	glyceraldehyde 3-phosphate
alpha-Linolenic acid metabolism	69	1	0.738	1	1	phospholipase A2
JAK-STAT signaling pathway	165	2	1.764	1	1	Akt; interleukin 19
Renal cell carcinoma	71	1	0.759	1	1	Akt
Adherens junction	71	1	0.759	1	1	tyrosine-protein kinase Fyn
Acute myeloid leukemia	71	1	0.759	1	1	Akt
Tight junction	167	2	1.785	1	1	protein phosphatase 2 ; myosin heavy chain 9/10/11/14
GnRH secretion	72	1	0.770	1	1	Akt
Non-small cell lung cancer	72	1	0.770	1	1	Akt
Ether lipid metabolism	72	1	0.770	1	1	phospholipase A2
Melanoma	73	1	0.780	1	1	Akt
Ascorbate and aldarate metabolism	76	1	0.812	1	1	2-oxoglutarate
Chronic myeloid leukemia	77	1	0.823	1	1	Akt
Glioma	78	1	0.834	1	1	Akt
Pancreatic cancer	78	1	0.834	1	1	Akt
Linoleic acid metabolism	78	1	0.834	1	1	phospholipase A2
Salmonella infection	79	1	0.845	1	1	rab-interacting lysosomal protein
Folate biosynthesis	83	1	0.887	1	1	7,8-dihydrobiopterin
Hepatocellular carcinoma	186	2	1.988	1	1	Akt; glutathione S-transferase
Neomycin, kanamycin and gentamicin biosynthesis	86	1	0.919	1	1	glucose 6-phosphate

B cell receptor signaling pathway	86	1	0.919	1	1	Akt
Gastric acid secretion	88	1	0.941	1	1	carbonic anhydrase 2
Viral myocarditis	88	1	0.941	1	1	tyrosine-protein kinase Fyn
ErbB signaling pathway	88	1	0.941	1	1	Akt
Colorectal cancer	89	1	0.951	1	1	Akt
Tuberculosis	195	2	2.085	1	1	lysosomal-associated membrane protein 2; Akt
Th1 and Th2 cell differentiation	90	1	0.962	1	1	notch2
Antigen processing and presentation	91	1	0.973	1	1	proteasome activator subunit 1
PD-L1 expression and PD-1 checkpoint pathway in cancer	92	1	0.984	1	1	Akt
TGF-beta signaling pathway	95	1	1.016	1	1	protein phosphatase 2
Salivary secretion	95	1	1.016	1	1	cGMP-dependent protein kinase 1
Nicotinate and nicotinamide metabolism	98	1	1.048	1	1	maleate
Insulin secretion	98	1	1.048	1	1	glucose 6-phosphate
Toll-like receptor signaling pathway	99	1	1.058	1	1	Akt
Morphine addiction	103	1	1.101	1	1	solute carrier family 32
Viral protein interaction with cytokine and cytokine receptor	103	1	1.101	1	1	interleukin 19
Rap1 signaling pathway	219	2	2.341	1	1	Akt; phospholipase C
Circadian entrainment	107	1	1.144	1	1	cGMP-dependent protein kinase 1
Choline metabolism in cancer	109	1	1.165	1	1	Akt
Prostate cancer	110	1	1.176	1	1	Akt
TNF signaling pathway	113	1	1.208	1	1	Akt

Ribosome biogenesis in eukaryotes	116	1	1.240	1	1	ribosome maturation protein SDO1
Tyrosine metabolism	118	1	1.262	1	1	maleate
Growth hormone synthesis, secretion and action	120	1	1.283	1	1	Akt
Natural killer cell mediated cytotoxicity	121	1	1.294	1	1	tyrosine-protein kinase Fyn
Cell cycle	123	1	1.315	1	1	14-3-3 protein epsilon
Staphylococcus aureus infection	123	1	1.315	1	1	complement component 5
Pathways in cancer	570	5	6.094	1	1	laminin B1; laminin; Akt; notch2; glutathione S-transferase
C-type lectin receptor signaling pathway	124	1	1.326	1	1	Akt
Yersinia infection	126	1	1.347	1	1	Akt
Tryptophan metabolism	130	1	1.390	1	1	3-hydroxyanthranilate
Relaxin signaling pathway	135	1	1.443	1	1	Akt
FoxO signaling pathway	136	1	1.454	1	1	Akt
Signaling pathways regulating pluripotency of stem cells	138	1	1.475	1	1	Akt
Estrogen signaling pathway	142	1	1.518	1	1	Akt
Measles	145	1	1.550	1	1	Akt
Apelin signaling pathway	146	1	1.561	1	1	Akt
Gastric cancer	154	1	1.646	1	1	Akt
Inflammatory mediator regulation of TRP channels	162	1	1.732	1	1	phospholipase A2
Hepatitis B	163	1	1.743	1	1	Akt
Arachidonic acid metabolism	164	1	1.753	1	1	phospholipase A2
MAPK signaling pathway	299	2	3.196	1	1	protein phosphatase 1A; Akt

MicroRNAs in cancer	303	2	3.239	1	1	fascin 1; notch2
Influenza A	169	1	1.807	1	1	Akt
RNA transport	169	1	1.807	1	1	eIF-4E
Drug metabolism - cytochrome P450	169	1	1.807	1	1	glutathione S-transferase
Cell adhesion molecules (CAMs)	171	1	1.828	1	1	sialoadhesin
Ribosome	174	1	1.860	1	1	ribosomal protein L36
Axon guidance	181	1	1.935	1	1	tyrosine-protein kinase Fyn
Necroptosis	186	1	1.988	1	1	ferritin heavy chain
Steroid hormone biosynthesis	188	1	2.010	1	1	7 beta-estradiol 17-dehydrogenase
Metabolism of xenobiotics by cytochrome P450	188	1	2.010	1	1	glutathione S-transferase
Cellular senescence	190	1	2.031	1	1	Akt
Chemical carcinogenesis	194	1	2.074	1	1	glutathione S-transferase
Chemokine signaling pathway	203	1	2.170	1	1	Akt
NOD-like receptor signaling pathway	215	1	2.298	1	1	14-3-3 protein epsilon
Kaposi sarcoma-associated herpesvirus infection	221	1	2.363	1	1	Akt
Regulation of actin cytoskeleton	221	1	2.363	1	1	myosin heavy chain 9/10/11/14
Viral carcinogenesis	231	1	2.470	1	1	14-3-3 protein epsilon
Epstein-Barr virus infection	232	1	2.480	1	1	Akt
Human immunodeficiency virus 1 infection	243	1	2.598	1	1	Akt
Neuroactive ligand-receptor interaction	402	2	4.298	1	1	glycine; complement component 5
Human T-cell leukemia virus 1 infection	251	1	2.683	1	1	Akt

Human cytomegalovirus infection	261	1	2.790	1	1	Akt
Endocytosis	275	1	2.940	1	1	vacuolar protein sorting 36
Herpes simplex virus 1 infection	439	2	4.693	1	1	complement component 5; Akt
Cytokine-cytokine receptor interaction	296	1	3.164	1	1	interleukin 19
Olfactory transduction	1141	1	12.198	1	1	cGMP-dependent protein kinase 1

Table S2.

Joint pathway analysis of cardiac metabolomics and proteomics.

Integrative analysis of proteomics (n=4) and metabolomics (n=5) data at pathway level of WT and MCJ^{KO} hearts. Differentially encountered metabolites (in orange) and proteins (in blue) were analyzed ($p<0.05$) by Joint Pathway Analysis using MetaboAnalyst 5.0.

Table S3.

Raw data.

Excel spreadsheet including all the raw data belonging to the graphs included in the manuscript.